Estuarine, Coastal and Shelf Science 171 (2016) 11–22

Contents lists available at ScienceDirect

Estuarine, Coastal and Shelf Science

journal homepage: www.elsevier.com/locate/ecss

Improved seagrass mapping using linear spectral unmixing of aerial photographs

Amy V. Uhrin [a, b, *], Philip A. Townsend [c]

[a] Department of Commerce, National Oceanic and Atmospheric Administration, National Ocean Service, National Centers for Coastal Ocean Science, Center for Coastal Fisheries and Habitat Research, 101 Pivers Island Road, Beaufort, NC 28516, USA
[b] University of Wisconsin-Madison, Department of Zoology, Ecosystem and Landscape Ecology Lab, 430 Lincoln Drive, Madison, WI 53706, USA
[c] University of Wisconsin-Madison, Department of Forest and Wildlife Ecology, 1630 Linden Drive, Russell Labs, Madison, WI 53706, USA

ARTICLE INFO

Article history:
Received 22 May 2015
Received in revised form
30 November 2015
Accepted 11 January 2016
Available online 13 January 2016

Keywords:
Seagrass spatial configuration
Seagrass classification
Linear spectral unmixing
Visual photointerpretation
Remote sensing
Digital aerial photography
North Carolina

ABSTRACT

Mapping of seagrass is challenging, particularly in areas where seagrass cover ranges from extensive, continuous meadows to aggregations of patchy mounds often no more than a meter across. Manual delineation of seagrass habitat polygons through visual photointerpretation of high resolution aerial imagery remains the most widely adopted approach for mapping seagrass extent but polygons often include unvegetated gaps. Although mapped polygon data exist for many estuaries, these are likely insufficient to accurately characterize spatial pattern or estimate area actually occupied by seagrass. We evaluated whether a linear spectral unmixing (LSU) classifier applied to manually-delineated seagrass polygons clipped from digital aerial images could improve mapping of seagrass in North Carolina. Representative seagrass endmembers were chosen directly from images and used to unmix image-clipped polygons, resulting in fraction planes (maps) of the proportion of seagrass present in each image pixel.

Thresholding was used to generate seagrass maps for each pixel proportion from 0 (no thresholding, all pixel proportions included) to 1 (only pixels having 100% seagrass) in 0.1 increments. The optimal pixel proportion for identifying seagrass was assessed using Euclidean distance calculated from Receiver Operating Characteristic (ROC) curves and overall thematic accuracy calculated from confusion matrices. We assessed overall classifier performance using Kappa statistics and Area Under the (ROC) Curve (AUC). We compared seagrass area calculated from each threshold map to the total area of the corresponding manually-delineated polygon. LSU effectively classified seagrass and performed better than a random classification as indicated by high values for both Kappa statistics (0.72–98) and AUC (0.80–0.99). The LSU classifier effectively distinguished between seagrass and bare substrate resulting in fine-scale seagrass maps with overall thematic accuracies that exceeded our expected accuracy target of 85% (range: 86.3–99.0%) and were comparable to those reported from previous seagrass mapping studies utilizing aerial image spectral data. The pixel proportion producing seagrass maps with highest accuracy varied among sites (range: 0 to 0.5). The optimal pixel proportion determined from Euclidean distance varied among sites (range: 0.2 to 0.6) and differed from those having highest accuracy. Importantly, the classifier identified small patches of seagrass, resulting in seagrass area estimates that were 2–94% lower than the area of the corresponding habitat polygon. We conclude that where seagrass polygon data exist, LSU can be used together with photointerpretation to generate spatially resolved maps suitable for analysis of seagrass spatial configuration and provide improved estimates of actual seagrass acreage.

Published by Elsevier Ltd.

1. Introduction

Seagrasses are widely recognized as sensitive indicators of overall estuarine health (i.e., high water quality), due in large part to light requirements that are higher than other estuarine primary producers (Dennison et al., 1993). Seagrass seascapes vary

* Corresponding author. Present address: Department of Commerce, National Oceanic and Atmospheric Administration, National Ocean Service, Office of Response and Restoration, Marine Debris Division, 1305 East-West Highway, SSMC4 Room 10-240, Silver Spring, MD 20910, USA.
E-mail addresses: amy.uhrin@noaa.gov (A.V. Uhrin), ptownsend@wisc.edu (P.A. Townsend).

http://dx.doi.org/10.1016/j.ecss.2016.01.021
0272-7714/Published by Elsevier Ltd.

substantially in extent and pattern and persist given a delicate balance between processes of disturbance and recovery (den Hartog, 1971; Fonseca et al., 1983). Seagrass seascapes display high spatial pattern heterogeneity, the result of localized hydrodynamic stress gradients (i.e., wind-wave exposure, tidal currents), and exhibit pattern-specific responses to acute disturbances like tropical cyclones (Fonseca and Bell, 1998; Fonseca et al., 2000; Gera et al., 2013; Pu et al., 2014). Large, contiguous seagrass meadows can develop in the absence of disturbance and in locations where current velocity, wave action, or biological disturbance (bioturbation) are relatively low. In contrast, numerous small seagrass patches characterize locations where storms are more frequent, or current velocity, wave action, and perhaps bioturbation are relatively high. In addition, seagrasses 'migrate' across the seascape in response to sedimentary processes including erosion and sediment accretion, leading to temporal pattern dynamics (Patriquin, 1975; Ferguson et al., 1993; Marba and Duarte, 1995; Ferguson and Korfmacher, 1997; Robbins and Bell, 2000; Fonseca et al., 2008). These patterns likely develop as a dynamic equilibrium (den Hartog, 1971; Patriquin, 1975; Fonseca et al., 1983; Fonseca and Bell, 1998; Koch et al., 2006; Walker et al., 2006).

The extent and pattern of seagrass seascapes influence both biological and physical functions of the broader seagrass ecosystem. Seagrass patch configuration and extent variably affect the distributions of a diverse assemblage of fauna (Turner et al., 1999; Boström et al., 2006, 2011), many with important commercial value (Thayer et al., 1984; Jackson et al., 2001; Heck et al., 2003). Patchy seagrass seascapes are vulnerable to seasonal bioturbation activities by sting rays that target the edges of intermediate-sized patches, exposing roots and rhizomes and leaving patches more susceptible to erosion (Townsend and Fonseca, 1998; Peterson et al., 2001). Seagrass patch spacing influences sediment resuspension, deposition, and erosion (Folkard, 2005) with implications for coastal stability and water quality. Seascapes characterized by patchy seagrass cover are more susceptible to loss of additional cover during extreme wind events (Fonseca et al., 2000; Gera et al., 2013). Seagrass coverage and pattern are relevant metrics for planning restoration projects (Fonseca et al., 1998). Moreover, given the link between disturbance and seagrass spatial heterogeneity (den Hartog, 1971; Patriquin, 1975; Fonseca et al., 1983; Fonseca and Bell, 1998; Koch et al., 2006; Walker et al., 2006), changes in the spatial configuration of a seagrass seascape may affect ecosystem resilience (*sensu* Holling's 'ecological resilience', 1973, 1996) and could serve as an indicator of system transition (Kéfi et al., 2014).

The spatially heterogeneous nature of most estuarine seagrass seascapes presents a challenge for accurately mapping this highly productive coastal resource. Visual interpretation of aerial photography remains the most widely adopted approach for mapping seagrass extent, including along the mid-Atlantic seaboard of the United States (Carroway and Priddy, 1983; Ferguson et al., 1993; Moore et al., 2000; Finkbeiner et al., 2001; Lathrop et al., 2006; Costello and Kenworthy, 2011). Visual interpretation involves hand-digitization of seagrass habitat boundaries while adhering to a minimum mapping unit (MMU), i.e. some smallest feature (e.g., an individual seagrass patch) or aggregate of features (e.g., scattered seagrass patches on sand) that provides a balance between generating maps with sufficient detail to meet the requirements of the end user and the time and cost to make the maps (Finkbeiner et al., 2001; Rohmann and Monaco, 2005). The high spatial resolution (sub-meter) of aerial images offers a distinct advantage over more widely available multi-spectral sensors, in terms of the visibility of fine-scale seagrass features. However, when seagrass patches are mapped as bounded aggregate features, substantial unvegetated substrate is found both between large, continuous seagrass beds and among smaller patches. As a result, a recognized limitation of this method is the inability to estimate the actual area of seagrass occupation in patchy habitats or to analyze fine-scale seagrass spatial pattern (Finkbeiner et al., 2001).

Another advantage of high resolution aerial images over those generated by some multi-spectral sensors is the reduction, but not elimination, of errors in classification accuracy due to mixed pixels (when features of interest are smaller than image spatial resolution; Woodcock and Strahler, 1987). Mixed pixels impede accurate habitat mapping because entire pixels are often assigned a single, unambiguous class membership (Smith et al., 1985; Pech et al., 1986; Settle and Drake, 1993; Fisher, 1997). Although mixed pixels continue to occur at boundaries between features regardless of feature size or sensor resolution (Schowengerdt, 2006), the issue can be alleviated by either using the finest resolution imagery available or employing spectral unmixing classifiers (Boyd and Foody, 2011). Spectral unmixing has been used to classify coral reefs from multi- and hyperspectral imagery (Hedley and Mumby, 2003; Mobley et al., 2005; Goodman and Ustin, 2007; Torres-Madronero et al., 2009; Hamylton, 2011). Applications to seagrass are few yielding mixed results for both hyper- and multi-spectral images (Meyer, 2008; Torres-Madronero et al., 2009).

Application of traditional image processing techniques to aerial images is challenging because individual image frames are often edge-matched for mosaicking to provide regional coverage, thus altering spectral data and precluding the development of consistent spectral signatures. We reviewed the range of digital image processing techniques used to classify seagrass from aerial images (Supplemental Data 1). The selection of a particular technique was location-dependent based on bathymetry, water clarity, seagrass spatial pattern, and neighboring habitats, and also limited by software accessibility and technical expertise. But overall, semi-automated and automated techniques increase overall accuracy compared to manual delineation alone (Supplemental Data 1).

The primary objective of this research was to evaluate the effectiveness of combining visual photointerpretation of high resolution digital aerial images (0.3 × 0.3 m) with a semi-automated linear spectral unmixing (LSU) classifier to improve mapping detailed seagrass spatial pattern in the shallow waters of the Albemarle-Pamlico Sound Estuary System in North Carolina. Specifically, we (1) determined whether a LSU classifier performed better than a random classification for all seagrass pixel proportions, (2) performed an accuracy assessment on seagrass fraction planes (maps) generated from LSU for all seagrass pixel proportions, (3) determined the optimal pixel proportion for labeling seagrass presence via LSU, and (4) evaluated whether the LSU classifier led to improved fine-scale seagrass maps by identifying small, individual seagrass patches and excluding bare substrate.

2. Methods

2.1. Study site description

The Albemarle-Pamlico Sound Estuary System is a coastal lagoon bordered on the east and south by a chain of barrier islands (Outer Banks). Broad shallows (<2 m deep at mean low water) are punctuated by deeper basins and channels. Seagrass beds along this portion of the North Carolina coast cover an area of ~554 km^2 behind the extensive barrier island system (APNEP, 2012). The beds are dominated by a mixture of the temperate seagrass *Zostera marina* (eelgrass) and the subtropical seagrass *Halodule wrightii* (shoal grass), with occasional *Ruppia maritima* (widgeon grass) in quiescent areas. Coastal North Carolina represents the only known overlapping acreage of *Z. marina* and *H. wrightii* in the world (Thayer et al., 1984).

Six sites were selected for evaluation located at the southern end of the Albemarle-Pamlico Sound Estuary System in two smaller sounds (Core and Back Sounds; Fig. 1). Seagrass seascapes in the subset were representative of cover types observed in the region, a result of hydrodynamic forcing (Fig. 2; Fonseca et al., 1983; Fonseca and Bell, 1998).

2.2. Image acquisition

On May 27, 2013, fixed-wing aerial imagery of the Albemarle-Pamlico Sound Estuary System was captured using the Zeiss/Intergraph Digital Mapping Camera interfaced to an Applanix Global Positioning System/Inertial Measurement Unit under optimal environmental conditions (e.g., wind speed, sun angle, tide stage, cloud cover, turbidity levels) following standard protocols for aerial imagery acquisition for the purposes of benthic habitat mapping in the region (Ferguson et al., 1993; Dobson et al., 1995; Finkbeiner et al., 2001). Images were collected in three bands: blue (410–490 nm), green (510–590 nm), and red (610–690 nm) at 1:25,400 scale and a sensor altitude of approximately 3048 m. A total of 242 individual 1524.39 × 1524.39 m images resulting from eight flight-lines provided coverage of the estuary.

Post-processing was performed by the North Carolina Department of Transportation Photogrammetry Unit. Images were orthorectified (5′ plain) and georeferenced to the North Carolina State Plane coordinate system, NAD 1983 (Conus) Datum at a 0.3048 m ground cell resolution and 8-bit radiometric resolution and provided as true color (3-band) digital image products in GeoTIFF format. Images were re-projected to the Universal Transverse Mercator coordinate system (Zone 18N), WGS 1984 Datum by staff at NOAA/NCCOS using the ERDAS® Imagine® software package and mosaicked by flight line.

2.3. Visual interpretation of seagrass

Seagrass beds were manually digitized following established protocols in ESRI® ArcMap™ (v. 10.2.1, Environmental Systems Research Institute, Redlands, CA) at a minimum mapping unit of 15 m on the longest axis. The digitizing scale was set between 1:2000 and 1:2500. The aerial images were viewed in a false-color scheme with a 2-standard deviation stretch of the red band (band 3) as red, the green band (band 2) as green, and the red band (band 3) again as blue.

Images were clipped to the extent of the digitized polygon feature to remove areas such as land, salt marsh, deep water, and manmade structures (e.g., docks, duck blinds) that may add noise to the classification procedure. For the purposes of this evaluation, linear spectral unmixing (LSU) was performed only on the individual clipped polygons that encompassed the six study sites. Limiting our seagrass classification to the extent of previously mapped polygons also eliminated tiling effects and variations in spectral response among frames, which may result when multiple image frames are mosaicked to achieve regional coverage.

2.4. Image pre-processing and endmember selection

Image pre-processing for the unmixing was conducted in ENVI (v. 5.0, Exelis Visual Information Solutions, Inc., McLean, VA). A forward Minimum Noise Fraction transformation (MNF, Green et al., 1988; Boardman and Kruse, 1994) was performed on each image to reduce spectral noise in the data and focus the spectral unmixing on the image information with most thematic content. MNF is a linear transformation that produces a set of principal component images ordered by decreasing signal quality. MNF divides the original data into two parts: one part associated with large eigenvalues and coherent eigenimages, and a complementary part with near-unity eigenvalues and noise-dominated images (Green et al., 1988; Boardman and Kruse, 1994). MNF bands were evaluated through visual inspection of the MNF band images and the resulting eigenvalue plots. Band images that appeared to be spatially coherent were selected. Estimation of the break in slope of the eigenvalue plot indicates a transition from bands containing

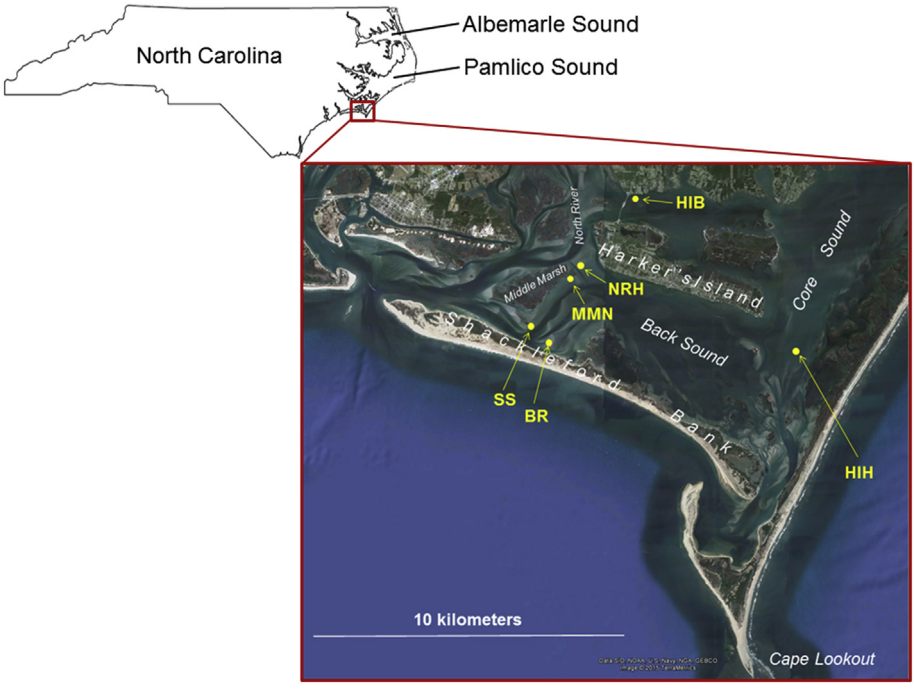

Fig. 1. Location of the six study sites in the southern region of the Albemarle-Pamlico Sound Estuary System, North Carolina (Back and Core Sounds). Site names are based on proximity to major geographic features. HIB: Harker's Island Bridge; NRH: North River High; MMN: Middle Marsh North; SS: Shackleford Shoal; BR: Bottle Run; HIH: Harker's Island High. Image from Google Maps (Data: SIO, NOAA, U.S. Navy, NGA, GEBCO; Image© Terrametrics).

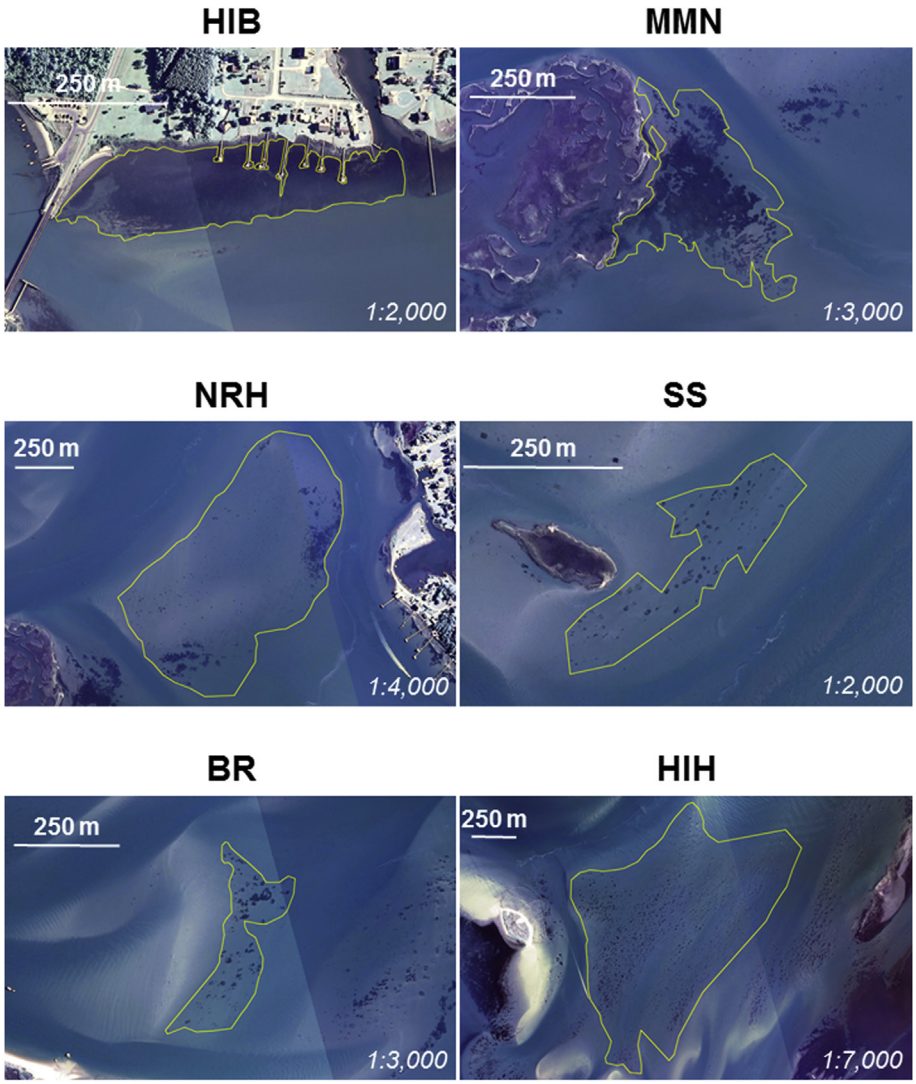

Fig. 2. Seagrass spatial patterns at six study sites located in Back and Core Sounds, North Carolina (2013 digital aerial imagery at 0.3 m resolution). The perimeters of visually interpreted seagrass polygons are indicated in yellow. The dark brown areas within the boundaries of each polygon are seagrass. (For interpretation of the references to colour in this figure legend, the reader is referred to the web version of this article.)

data (eigenvalue greater than one) and those that are predominantly noise (eigenvalues less than one). Band images whose eigenvalues were above the break in slope (greater than one) were selected to use in the unmixing along with the original red, green, and blue spectral bands, resulting in final images with five or six bands (R, G, B, MNF1, MNF2, and potentially MNF3), and thereby increasing image dimensionality.

Endmembers were manually identified in each individual image based on in-situ mapping efforts conducted at the study sites in summer 2013. Perimeters of existing seagrass patches located within 100 × 50 m sample plots were physically traced using differentially-corrected GPS (Trimble® GeoXH™, Trimble Navigation Ltd., Sunnyvale, CA). Given the high image resolution, availability of ground truth data, and results of a previous pilot study, we were confident that a one single seagrass endmember (chosen per individual image) was sufficient to characterize the spectral characteristics of submerged seagrass (Fig. 3). One limitation of LSU is that the number of endmembers used for classification cannot exceed the number of image bands. Therefore, the range of spectral variation in bare substrates in the images could not be accommodated as multiple endmembers. The number of unique endmembers used to characterize spectrally differing examples of bare substrate varied among the images due to differences in sun glint and sediment composition. In some instances bare substrate composition was consistent throughout an image and easily represented by one endmember. In other cases, the remaining available endmembers were insufficient. In these situations, endmembers were selected to represent bare substrate components comprising the largest areal coverage in an image.

2.5. Linear spectral unmixing (LSU)

In LSU, the measured spectrum of a mixed pixel is decomposed into its constituent spectra, or endmembers and a set of corresponding image fractions that indicate the proportion of each endmember present in the pixel are generated. Thus, vegetation endmember fractions are proportional to the areal abundance of projected canopy cover (Roberts et al., 1993; Williams and Hunt, 2002). LSU operates under the following assumptions (Settle and Drake, 1993):

1) each endmember is known;
2) multiple scattering between the different endmembers is negligible;

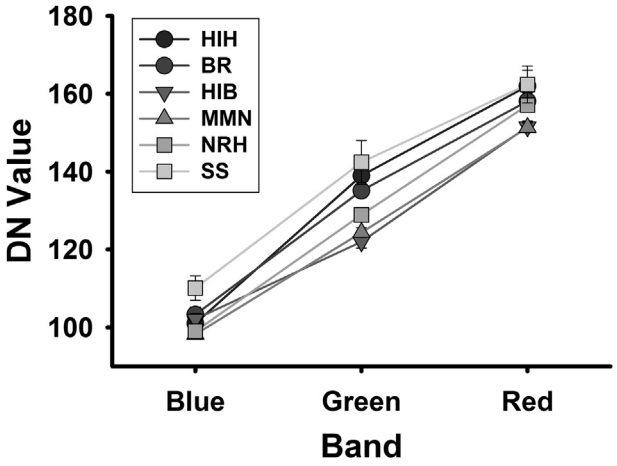

Fig. 3. Mean (±SD) digital number (DN) values for each image band (B:G:R) in each seagrass endmember identified in the 2013 aerial imagery for each study site.

3) endmembers are sufficiently spectrally contrasted so as to allow separation; and
4) a pixel is a linear combination of its constituent endmembers.

Unmixing algorithms are commonly based on variants of the linear mixture model:

$$R_x = \sum_{i=1}^{n} a_{xi} f_i + \varepsilon_x,$$

where R_x = the reflectance of a given pixel in the xth of z spectral bands, n = the number of mixture components (i.e., cover types), f_i = the fractional component of endmember i, a_{xi} = the reflectance of endmember i in spectral band x, and $\mathcal{E}_x$ = the error at spectral band x. LSU is subject to two constraints on f: the nonnegativity condition and the full additivity condition. To be physically meaningful, all image fractions must be nonnegative ($0 \leq f_i \leq 1$), and to account for the entire image composition, the image fractions must sum to unity ($f_1 + f_2 + \ldots f_i = 1$).

LSU was performed on the 5- or 6-band images using a unit sum constraint. Undershoots (negative proportions) and overshoots (superunity proportions) are common in unmixed fraction images due to imperfect endmembers (*sensu* Mather, 1999; Duran and Petrou, 2009). Close inspection of the fraction images revealed that only a small percentage of pixels exhibited superunity; however, negative fraction values occurred frequently, predominantly in areas of high root mean square error (RMS) that coincided with unvegetated substrates having very high reflectance, likely a result of the combination of water depth (near exposure) and sediment composition (coarse sand). As these areas were not of interest in the study, all bands were truncated using band math so that any negative values were assigned to be zero (Brandt and Townsend, 2006). The bands were then rescaled by dividing by the largest fraction value so that all endmembers for a pixel summed to unity (Brandt and Townsend, 2006).

2.6. Pixel proportion threshold approach

We used a threshold approach (Arnot et al., 2004; Frazier and Wang, 2011) to transform the sub-pixel seagrass fraction plane data into a discrete format. Statistics generated from the seagrass fraction plane were used to build masks (selected areas = "on") by grouping pixels with values greater than or equal to the threshold. The initial mask (proportion = 0) included all pixels containing seagrass, no matter the pixel proportion (i.e., no threshold). Subsequent masks were generated in 0.1 increments of seagrass proportion from the unmixed seagrass fraction planes. The individual mask layers (seagrass maps generated by unmixing) were exported to ArcMap™ as rasters for construction of error matrices.

2.7. Accuracy assessment

Thematic accuracy of seagrass presence/absence was evaluated using an error matrix generated for each 0.1 proportion increment from the unmixing procedure, by individual site as well as for all sites combined. The matrix evaluated the ability of unmixing to distinguish seagrass elements versus non-seagrass elements (substrate). Given the binary nature of the resulting classified maps, the appropriate sample size for assessing thematic accuracy was derived from the formula for binomial probabilities as suggested by Fitzpatrick-Lins (1981):

$$\mathrm{N} = \frac{Z^2(p)(q)}{E^2}$$

where p is the expected percent accuracy of the entire map, q = 100- p, E is the allowable error, and Z = 2 from the standard normal deviate of 1.96 for the 95% two-sided confidence level. Here, we set expected accuracy to 85%, which is a commonly accepted overall thematic accuracy target (Thomlinson et al., 1999; Jensen, 2005; Congalton and Green, 2009).

Therefore, with an expected accuracy of 85% at an allowable error rate of 5%, and rounding up to ensure an equal number of samples in each class, the formula indicated that a minimum of 204 reference points were necessary for a reliable error matrix (102 for each class).

Field data for accuracy assessment were collected June–September 2013. At each of the six sites, the outline of every seagrass patch present within one 100 × 50 m plot per site was traced using the differentially-corrected GPS. Perimeters were delineated irrespective of proportion of seagrass, meaning that all patches contained seagrass, but percent cover was not recorded within individual patches. Using ArcMap™ (v. 10.2.1), stratified random reference points for seagrass (25) and sand (25) were generated from within the boundaries of the 100 × 50 m plots. The remaining reference points (75 for each class) were randomly distributed within the larger boundary of the associated manually digitized seagrass site polygon.

2.8. Classifier performance

The performance of the LSU classifier was evaluated using two criteria: the Kappa statistic ($\hat{K}$) and the Area Under the Curve (AUC). Both methods assess whether the LSU classifier performed better than a random classification.

2.8.1. Kappa statistic ($\hat{K}$)

Kappa ($\hat{K}$) was computed for each error matrix following the procedure of Congalton et al. (1983) using PROC FREQ in SAS® (v. 9.4, SAS Institute Inc., Cary, NC). $\hat{K}$ is a measure of how well a classification agrees with reference data. Values for $\hat{K}$ range between −1 and 1 but positive values are expected because the classification and the reference data are positively correlated. As a rule of thumb, strong agreement between the classifier and the reference data is indicated by $\hat{K} > 0.80$ while moderate agreement is indicated by $\hat{K}$ in the range 0.40–0.80 (Landis and Koch, 1977). Z statistics were used to determine if the LSU classifier performed better than a random classification (i.e., $\hat{K}$ significantly greater than zero).

2.8.2. Area Under the Curve (AUC)

Receiver Operating Characteristic (ROC) curve analysis was conducted using PROC LOGISTIC in SAS® to evaluate the performance of the LSU classifier as the pixel proportion of seagrass was varied. A ROC curve is a plot of sensitivity (true positive rate) versus 1 minus specificity (false positive rate) for all pixel proportions and describes the tradeoffs between the accurate detection and false detection of seagrass. An optimum classification model would be one with the highest possible value of sensitivity and specificity, minimizing omission and commission errors at the same time. The chance performance of a model lies on the positive diagonal of a ROC plot, whereas models that out-perform chance follow a curve lying in the upper left half. Therefore, pixel proportions appearing on the left-hand side of an ROC curve, near the x-axis may be thought of as "conservative" where positive classifications are made only with strong evidence, so few false positive errors are made, but true positive rates are low as well. Pixel proportions on the upper right-hand side of an ROC curve may be thought of as "liberal" where positive classifications are made with weak evidence, so nearly all positives are classified correctly but false positive rates are high as well. Individual ROC curves were generated for each study site as well as a combined curve using data summed across the sites.

The overall performance of LSU at all pixel proportions for individual sites and for all sites combined was assessed using PROC FREQ in SAS® to determine the total area under the ROC curve (AUC). AUC ranges from 0.5 to 1.0 where 0.5 represents the positive diagonal and is indicative of a classifier that performs no better than random. Higher values of the AUC indicate better classifier performance where 1.0 indicates a perfect classification.

2.9. Seagrass map thematic accuracy

Overall thematic accuracy was computed for each error matrix in addition to errors of commission and omission, producer's accuracy, and user's accuracy (Story and Congalton, 1986). Our overall thematic accuracy target was set to 85%, which is a commonly accepted target in the literature (Thomlinson et al., 1999; Jensen, 2005; Congalton and Green, 2009).

2.10. Optimal pixel proportion

To evaluate the optimal pixel proportion, or the proportion that would make the resulting seagrass prediction as close to a perfect predictor as possible, we calculated the Euclidean distance (d) between the specificity (x) and sensitivity (y) pair for each pixel proportion threshold on the ROC curve and the (x,y) coordinate for a perfect classification (0, 1) as:

$$d = \sqrt{(x_1 - x_2)^2 + (y_1 - y_2)^2}$$

where (x_1, y_1) is the perfect classification pair of (0,1) and (x_2,y_2) is the specificity and sensitivity pair for the pixel proportion under evaluation. Euclidean distances across pixel proportion thresholds were then compared; the optimal pixel proportion was that proportion having the shortest Euclidean distance.

2.11. Seagrass area comparison

The area of seagrass within each seagrass fraction plane threshold was calculated by summing the total number of seagrass pixels within each fraction plane and multiplying by the pixel area (here, 0.09 m^2). Areas of the manually digitized polygons were calculated in ArcMap™.

We anticipated *a priori* that the calculated area of seagrass classified from within the manually mapped polygon would decrease as pixel proportion increased (became more restrictive). In addition, the data violated assumptions of normality and homogeneity of variance. Therefore, Page's (1963) nonparametric trend test (Conover, 1999) followed by post hoc comparisons (Ipe, 1987) using the Bonferroni adjustment for multiple comparisons were performed using PROC GLM in SAS® to compare differences in seagrass area between each pixel proportion threshold and the total area of the manually mapped polygon.

3. Results

3.1. Classifier performance

The linear spectral unmixing (LSU) classifier performed better than a random classification for all pixel proportions (all $\widehat{K}$ significant at $p < 0.0001$; all AUC significant at $p = 0.05$; Table 1; Fig. 4). $\widehat{K}$ ranged from 0.72 to 98 (combined sites: 0.75) indicating moderate to strong agreement between reference data and the LSU classifier. AUC was high ranging from 0.80 to 0.99 (combined sites: 0.87), indicating that $\geq$ 80% of randomly chosen pairs of pixels (one seagrass, one sand) would be correctly classified by the unmixing classifier (Table 1; Fig. 4).

3.2. Seagrass map thematic accuracy

For all sites, the seagrass map with highest overall thematic accuracy as generated using LSU, exceeded the 85% accuracy target (Table 1). The pixel proportion producing the highest accuracy site map varied among sites (Table 1; Fig. 5). Highest overall accuracy ranged from 86.3 to 99% across the sites (combined sites: 87.7%) and corresponded to pixel proportions ranging from 0 to 0.5 (combined sites: 0.1; Table 1). Combined confusion matrix data yielded highest accuracy at a pixel proportion of 0.1 (Table 1; Fig. 5).

3.3. Optimal pixel proportion

Optimal pixel proportions determined using Euclidean distance calculations varied across the six sites, ranging from 0.2 to 0.6, and were not the same pixel proportions as those having the highest overall thematic accuracy (Table 1; Figs. 4–6). The combined site data resulted in an optimal pixel proportion of 0.4 (Table 1; Fig. 4.). Consultation with the original confusion matrix revealed that these optimal pixel proportions were associated with lower overall accuracies and lower $\widehat{K}$ (Table 1; Figs. 4–6). Overall accuracies for the optimal pixel proportions at each site ranged from 62.7 to 92.6% (combined sites: 66.3%) and kappa values ranged from 0.25 to 0.85 (combined sites: 0.25; Table 1).

3.4. Seagrass area comparison

Estimates of seagrass area from maps based on the pixel proportion yielding the highest overall thematic accuracy were 2–94% lower than the area of the corresponding manually delineated polygon (Table 1). The area classified as seagrass via LSU declined linearly with increasing pixel proportion; all cross-proportion comparisons were significantly different from one another and from the manually delineated polygon (Supplemental Data 2; $p = 0.05$ for all comparisons).

4. Discussion

Our study directly addresses limitations associated with established photointerpretation methods for mapping seagrass extent,

Table 1
Optimal pixel proportion, overall thematic accuracy, Kappa statistics ($\widehat{K}$), Area Under the Curve (AUC), and % decrease in area classified as seagrass (when compared to the corresponding manually delineated polygon) by site as determined using highest overall accuracy and Euclidean distance. "." indicates where metric calculation is not possible given the selection criterion under evaluation.

Site	Pixel proportion	Overall thematic Accuracy	$\widehat{K}$	AUC	% Decrease in Seagrass Area
Based on Euclidean distance from ROC curves					
HIB	0.3	62.7	0.25	0.97	46.8
MMN	0.4	75.5	0.50	0.93	60.0
NRH	0.4	71.1	0.42	0.95	96.0
HIH	0.2	68.6	0.37	0.99	98.4
BR	0.3	74.0	0.48	0.99	98.5
SS	0.6	92.6	0.85	0.80	96.3
COMBINED	0.4	66.3	0.25	0.87	.
Based on highest thematic accuracy from error matrices					
HIB	0	89.7	0.79	.	2.1
MMN	0.2	86.3	0.72	.	41.3
NRH	0.2	88.2	0.76	.	91.5
HIH	0.1	97.1	0.94	.	93.7
BR	0.1	99.0	0.98	.	90.2
SS	0.5	93.6	0.87	.	94.0
COMBINED	0.1	87.7	0.75	.	.

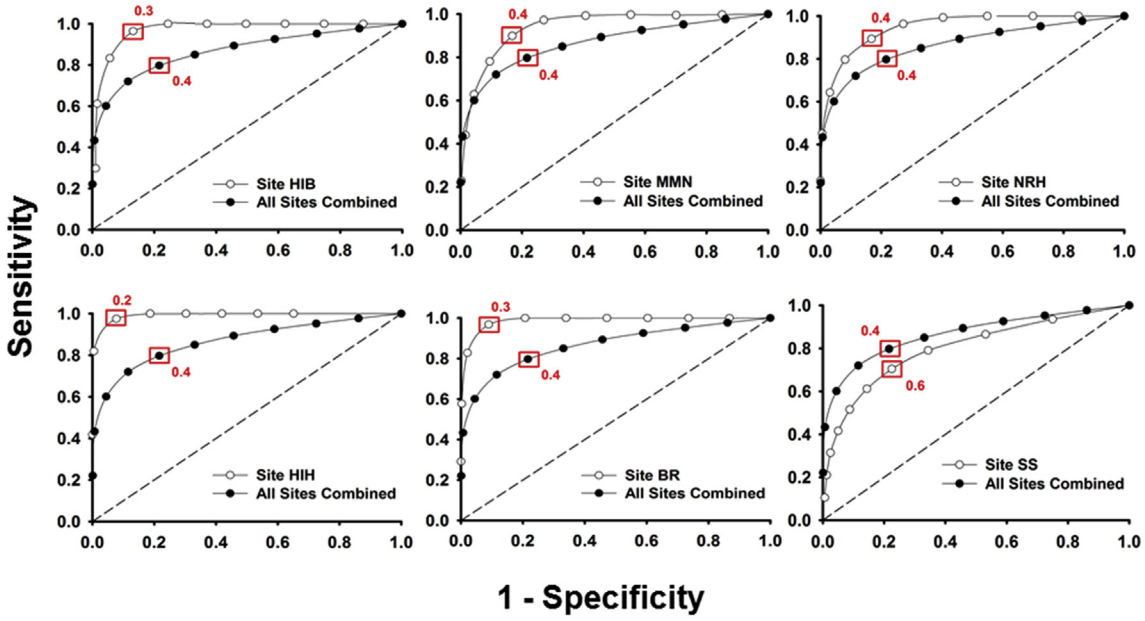

Fig. 4. Receiver Operating Characteristic (ROC) curves for the classification of seagrass at six study sites. The diagonal line represents a model with no predictive ability (AUC = 0.5). Individual points on the curve represent thresholds of seagrass pixel proportion in increments of 0.1 beginning with all proportions of seagrass included (no threshold) and ending with only those pixels containing 100% seagrass (threshold of 1.0). ROC curves for individual sites are indicated by open circles while curves generated using combined site data are indicated by filled circles. Red boxes denote the optimal pixel proportion threshold as suggested by Euclidean distance calculations. (For interpretation of the references to colour in this figure legend, the reader is referred to the web version of this article.).

in particular the inability to assess spatial configuration or to quantify actual area occupied by seagrass in patchy seascapes. We have demonstrated that linear spectral unmixing (LSU) effectively classified seagrass and performed better than a random classification as indicated by high (and significant) values for both Kappa statistics (0.72–98) and Area Under the Curve (0.80–0.99). LSU effectively distinguished between seagrass and bare substrate resulting in fine-scale seagrass maps with overall thematic accuracies that exceeded our expected accuracy target of 85% (range: 86.3–99.0%). By identifying small, individual seagrass patches and eliminating bare substrate from within the boundaries of manually mapped seagrass polygons, the LSU classifier effectively improved seagrass maps, moving beyond 'seagrass habitat' extent and allowing for estimation of actual seagrass area. Moreover, our results revealed that if LSU were not applied and manually mapped seagrass habitat extent were considered equivalent to the actual area of seagrass occupation (as has been done in the past), area would be greatly overestimated by anywhere from 70 to 1572% in patchy seagrass seascapes.

Linking landscape pattern and process requires an understanding of both the spatial and temporal dynamics of that pattern to develop a sense of what is typical at a given location (Gustafson, 1998). Seagrass maps generated from unmixing provide the data necessary to characterize fine-grained spatial pattern using landscape configuration metrics (e.g., McGarigal and Ene, 2013), a key step in building a predictable and ultimately, causal relationship between pattern and process. Not unlike terrestrial systems, the spatially heterogeneous nature of seagrass seascapes influences a

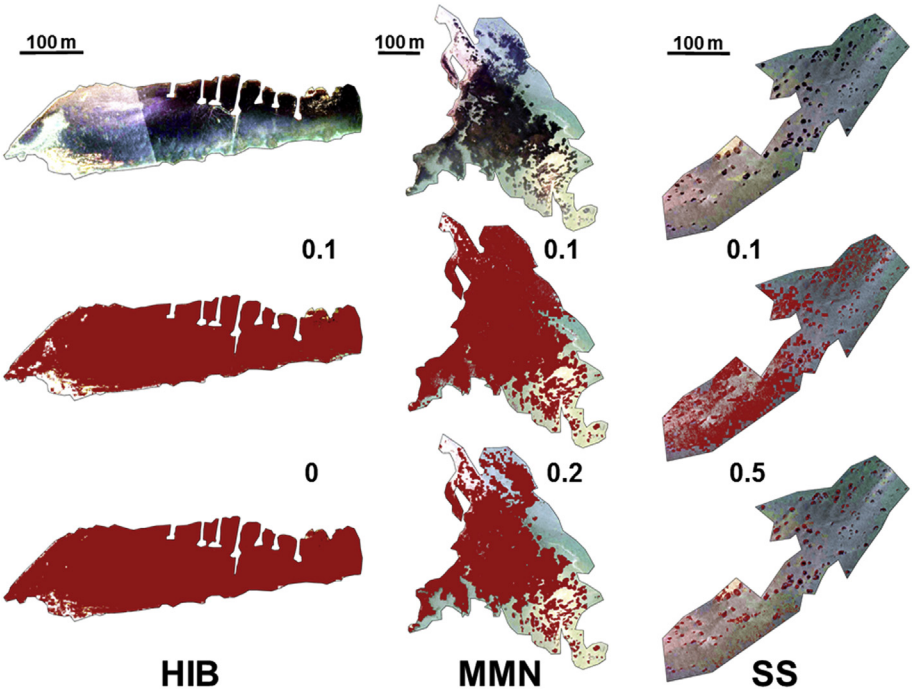

Fig. 5. Seagrass fraction planes generated from linear spectral unmixing for three representative sites: continuous seagrass (HIB); elongated seagrass patches grading into a continuous bed (MMN); small widely-dispersed patches (SS). Polygons in the top row were manually delineated via visual photointerpretation. In the middle row, the photo interpreted seagrass polygon is overlain with the optimal pixel proportion layer as suggested by highest overall thematic accuracy for the combined data. In the bottom panel, the photo interpreted seagrass polygon is overlain with the optimal pixel proportion as suggested by highest overall thematic accuracy within an individual site. Red-colored pixels are those pixels classified as seagrass by the linear spectral unmixing procedure. (For interpretation of the references to colour in this figure legend, the reader is referred to the web version of this article.).

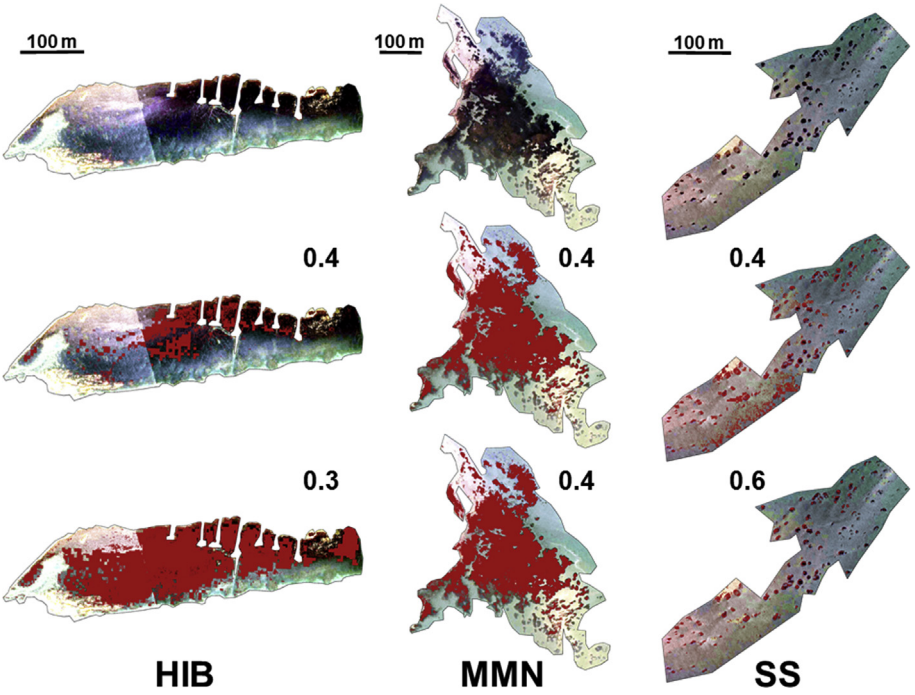

Fig. 6. Seagrass fraction planes generated from linear spectral unmixing for three representative sites: continuous seagrass (HIB); elongated seagrass patches grading into a continuous bed (MMN); small widely-dispersed patches (SS). Polygons in the top row were manually delineated via visual photointerpretation. In the middle row, the photo interpreted seagrass polygon is overlain with the optimal pixel proportion layer as suggested by Euclidean distance for the combined data. In the bottom panel, the photo interpreted seagrass polygon is overlain with the optimal pixel proportion as suggested by Euclidean distance within an individual site. Red-colored pixels are those pixels classified as seagrass by the linear spectral unmixing procedure. (For interpretation of the references to colour in this figure legend, the reader is referred to the web version of this article.)

number of biological and physical functions, including the distribution of organisms, bioturbation rates, and sediment erosion

and deposition, which may be altered if spatial configuration is modified (Townsend and Fonseca, 1998; Turner et al., 1999; Peterson et al., 2001; Folkard, 2005; Boström et al., 2006, 2011). Changes in the configuration of a seagrass seascape over space and time may also affect ecosystem resilience (*sensu* Holling's 'ecological resilience', 1973, 1996) and pattern-based spatial indicators have been suggested for identifying a system on approach to a critical transition (e.g., observed changes in patch-size distributions as vegetation shifts from continuous to patchy to bare substrate; Kéfi et al., 2014). The unmixing technique may be applied to available historical imagery to characterize seagrass pattern on temporal scales, determine change, and establish historical range of variability (Swetnam et al., 1999; Keane et al., 2009). Knowing the historical range of variability for seagrass pattern enables assessment of whether present day seagrass seascape configuration is within the historical range or represents an outlier seascape configuration that may indicate the beginnings of a regime shift to an unvegetated state (*sensu* Scheffer and Carpenter, 2003; Kefi et al., 2014). Additionally, knowledge of the historical range of variability with regard to seagrass seascape pattern can also help establish realistic restoration project goals and guide appropriate spatial configurations for restoration (Bell et al., 1997; Fonseca et al., 1998).

Seagrass maps generated from LSU facilitate estimates of actual seagrass acreage providing fishery managers with improved inventories of the amount of seagrass vegetation available for utilization by a diverse assemblage of species having ecological, recreational, and commercial importance. Faunal density and number of species are significantly higher in seagrass compared to unvegetated substrate (Heck et al., 2003 and references therein). This increased abundance includes a number of important fishery species that access seagrass at some stage of their life cycle as a nursery, feeding, or spawning area or shelter from predation (Thayer et al., 1984; Jackson et al., 2001; Heck et al., 2003). Seagrasses have also been reported to contribute disproportionately to the total annual landings value of some commercial fisheries (Jackson et al., 2015). These authors found that seagrass-associated species in the Mediterranean contributed 35% to the total landings value of commercial fisheries (CVF). When seagrass residence time for each fishery species was indexed and applied, four of 35% of CVF was directly attributed to the presence of seagrass, despite seagrass covering only 2% of the Mediterranean seafloor (Jackson et al., 2015). Thus, accurate inventories of seagrass acreage are fundamental in determining the direct contribution of seagrass to fisheries production as well as the potential loss of production due to seagrass decline.

The potential for using spectral data from aerial images for seagrass classification and mapping has been demonstrated in a number of studies and the high overall accuracies achieved in this study are comparable to those reported elsewhere using alternative approaches (Supplemental Data 1). Unfortunately, only half of the identified studies reported overall thematic accuracy. The remainder either provided no accuracy assessment or derived a metric unique to the study. This lack of standardization in accuracy reporting (or no reporting at all) is a common issue in the classification of remotely sensed data and limits operational application and comparative analysis (Congalton, 1991; Foody, 2002). None of these other studies utilized LSU, precluding direct comparison with our findings. However, an emerging theme across all studies is the opportunistic nature of seagrass mapping efforts, a result of spatial and temporal limitations in many regional image data sets likely due to a lack of sustained monitoring programs oftentimes driven by the cost associated with acquiring images. This lack of consistent, comparative information poses a challenge for resource managers who must weigh the trade-offs between working with potentially suboptimal data versus foregoing efforts to map/inventory the local seagrass resource. Taken together, these studies suggest that there is no universally applicable classification scheme for seagrass; selection of a classifier is ultimately dictated by several factors. These factors include the locale under study (i.e., seagrass spatial configuration, water clarity, sediment composition), availability of imagery (temporal and spatial limitations), type and quality of available imagery (i.e., high versus low resolution, aerial versus multi- or hyperspectral, presence of sun glint), software accessibility, technical support, and the specific survey questions being addressed (i.e., extent, spatial pattern, change detection).

Some elements of image interpretation such as texture (characteristic placement and arrangement of repetitions of tone or color), situation (how image features are organized and oriented relative to one another) and association (related features or phenomena are present) cannot be consistently programmed and automated (Jensen, 2006). Therefore, accurate habitat classification necessitates some level of visual evaluation (Finkbeiner et al., 2001; Meehan et al., 2005; Lathrop et al., 2006; Field, 2007; Fletcher et al., 2009; Young et al., 2010). The ability to visually identify and mask unwanted image features such as deep water channels, land, anthropogenic features (i.e., docks) and to constrain the LSU classifier to polygons of known seagrass habitat were key steps in our analysis in order to avoid classification error; such constraints have been recognized by others as essential for effectively mapping patchy seagrass (Green and Lopez, 2007).

Among sites, the seagrass proportion that yielded the most accurate classification differed between the Euclidean distance (ROC curve) and confusion matrix approaches due to differences in how the metrics are calculated. In contrast to counts of true/false positives/negatives as in a confusion matrix, ROC curve analysis is based on calculation of the predicted probabilities of an event occurring (seagrass being present) for each pixel proportion. Therefore, final selection of an optimal pixel proportion for the classification of seagrass required analyst knowledge of the system, i.e. what is a reasonable amount of seagrass that would constitute a "true positive". Final selection of an optimal pixel proportion also represents tradeoffs among overall thematic accuracy and the costs of failing to detect positives against the costs of falsely classifying a location as seagrass. Articulation of the analyst's designation of a "true positive" is another challenge for achieving among-project consistency.

Ground truth or validation data may not be accessible or attainable for every image frame or mapped polygon in a classification analysis of aerial imagery. Absence of such data limits determination of optimum pixel proportion. By merging confusion matrix data from the six sites, we provided a best compromise pixel proportion for situations when robust validation data are not available. However, final selection of an optimal pixel proportion would require visual evaluation by the analyst as the optimal pixel proportion chosen within a geographic area will vary depending upon which selection method is used (ROC Euclidean distance versus highest overall accuracy). Similarly, the proportion of seagrass with best performance (highest overall accuracy) differed among sites depending upon which selection criterion was used. Multiple, parallel flight lines with end-lap and side-lap of individual frames are required to provide full coverage of the Albemarle-Pamlico Sound Estuary System. As a result, individual frames may experience slight variations in sun angle and hence, sun glint, as an overflight progresses. Glint is minimized when standard acquisition protocols are followed [i.e., wind speed (0–8 kph), sun angle (30–45°); Ferguson et al., 1993; Dobson et al., 1995; Finkbeiner et al., 2001] and sun glint did not appear to be an issue in the 2013 imagery. Constraining our analysis to areas of known seagrass presence further limited the potential inclusion of glint by reducing

the total amount of image area used in the analysis, including areas over open water where glint is most pervasive. Most of our study sites were not co-located within image frames and the position of study sites within a single frame (proximity to frame edge) varied. Therefore, subtle spectral differences among sites with corresponding differences in optimal pixel proportion are not surprising.

Changes in water depth during image acquisition may also influence the classification of seagrass from aerial imagery. When acquiring aerial imagery for seagrass classification, published criteria for tidal stage recommend that overflights should occur within 2 h of the lowest predicted tide, thus reducing both water column thickness and associated errors due to scattering (Ferguson et al., 1993; Dobson et al., 1995; Finkbeiner et al., 2001). Still, differences in tide stage occur within the course of a single overflight, creating the potential for differences in bottom reflectance due to variable water depth among image frames and hence across sites. Water column correction techniques have been used to allow depth invariant processing of imagery (e.g., Lyzenga, 1978, 1981) and may improve estimates of bottom reflectance and hence classification accuracy in shallow-water marine systems Zoffoli et al. (2014). However, depth invariant corrections require that the same benthic habitat occur over a wide range of depth and the associated algorithms rely on subtracting a deepwater value from each pixel. These corrections are poorly suited for the shallow seagrass meadows of North Carolina where seagrass does not occur below 2 m depth (max water depth for sites used in this study: 1.3 m). Thus, although a shallow-water layer may remain over some sites at low tide, water column scattering or differences in bottom reflectance due to variable depth were presumed negligible and undeserving of depth invariant processing (Mount, 2006; Zhang et al., 2013). In fact, for shallow (0–3 m) temperate seagrass habitats in Tasmania, Mount (2006) observed sand to be readily distinguishable from submerged aquatic vegetation whether depth correction was applied or not and depth-corrected imagery "produced no discernible improvement in the accuracy of the SAV density maps."

Sediment composition and associated differences in spectral reflectance may also influence the classification of seagrass from aerial imagery. Here, sediment composition at patchy sites consisted of a greater proportion of coarse sand versus silt/clay than sites with larger more elongate patches or continuous seagrass cover (Fonseca and Bell, 1998). Coarse sand has a higher bottom reflectance than silt/clay sediments and seagrass (Maritorena et al., 1994; Werdell and Roesler, 2003). Although we did not attempt to distinguish among sediment constituents, differences in bottom reflectance, and hence optimum pixel proportions across sites, may also be related to variations in sediment texture.

In North Carolina, environmental conditions (e.g., wind speed, cloud cover) meeting standard acquisition requirements for aerial imagery typically occur during the spring (late April to early June) before the onset of summer haze, increased water column turbidity associated with runoff, and the potential for tropical cyclone activity all of which can interfere with image quality. This timing coincides with peak seasonal biomass of subtidal *Zostera marina*, one of the two co-dominant seagrass species in the Albemarle-Pamlico Sound Estuary System (Kenworthy, 1981). *Halodule wrightii* occurs as monospecific beds in the intertidal but often mixes with eelgrass in deeper water, peaking in late summer and fall and contributing substantially to total plant biomass (Kenworthy, 1981). Consequently, continuous seagrass cover is achieved throughout most of the year in the Albemarle-Pamlico Sound Estuary System. From a resource mapping perspective, the choice of season in which to conduct imagery acquisition represents a trade-off between obtaining the best possible quality imagery in a given year versus accurately capturing the seasonal maximum of a given species.

5. Conclusion

Seagrass mapping efforts are often opportunistic and are dependent on the spatial and temporal availability of imagery across regions. Moreover, there is no universally-applicable classification technique for seagrass. As a result, some analyst interpretation of high-resolution imagery will almost always be needed to select unique training areas in different images to account for spectral differences due to sun angle and tides. Ultimately, selection of a classifier is dictated by several factors including environmental parameters, availability of imagery, type and quality of imagery, software accessibility, technical support, and the specific survey questions being addressed.

Although coarse polygon data describing seagrass distribution exist for many estuarine areas, these are rarely sufficient to accurately characterize seagrass acreage or spatial pattern, as illustrated by our results indicating potentially large overestimations of seagrass area when maps are generated using photointerpretation. We demonstrate that a semi-automated linear spectral unmixing classifier can substantively improve seagrass mapping in shallow waters of the Albemarle-Pamlico Sound Estuary System in North Carolina by correctly identifying small seagrass patches, thus providing spatially resolved maps suitable for analysis of seagrass spatial configuration and estimation of seagrass acreage. A key step in the procedure reported here was the masking of unwanted image features by using existing mapped polygons to constrain the classifier to known areas of seagrass habitat.

Our approach will likely be useful in other estuarine systems where seagrass distribution is depth-limited (i.e., shallow) and the seascape is composed of a mixture of highly contrasted cover types (i.e., seagrass versus sand). In particular, the mapping of seagrass pixel proportions using unmixing will facilitate using ROC curves and confusion matrices to determine appropriate levels of proportional cover, correctly distinguishing locations of seagrass cover from areas where it is absent.

Acknowledgments

Funding was provided by the NOAA National Ocean Service Coastal Science Board with indirect support from the National Centers for Coastal Ocean Science and the University of Wisconsin-Madison. Aerial imagery was generously provided by the Albemarle-Pamlico National Estuary Partnership. We thank X. Liu, M. Ozdogan, R. Phetteplace, and B. Spaier for technical assistance. We benefited from discussion with P. Blank, J. Brandt, E. Erdmann, M. Fonseca, M. Garcia, R. Graves, B. Harvey, M. Jackson, J. Qiu, and T. Whitby. The manuscript was strengthened by comments from D. Field, M. Finkbeiner, C. Hu, P. Marraro, M. Turner, J. Zedler and two anonymous reviewers assigned by the journal. The views expressed here do not necessarily reflect those of NOAA.

Appendix A. Supplementary data

Supplementary data related to this article can be found at http://dx.doi.org/10.1016/j.ecss.2016.01.021.

References

APNEP (Albemarle-Pamlico National Estuary Partnership), 2012. 2012 Albemarle-Pamlico Ecosystem Assessment. Albemarle-Pamlico National Estuary Partnership. North Carolina Department of Environmental Quality, Raleigh, North Carolina. http://portal.ncdenr.org/web/apnep/reports (accessed 22.12.15.).

Arnot, C., Fisher, P.F., Wadsworth, R., Wellens, J., 2004. Landscape metrics with ecotones: pattern under uncertainty. Landsc. Ecol. 19, 181–195.

Bell, S.S., Fonseca, M.S., Motten, L.B., 1997. Linking restoration and landscape ecology. Restor. Ecol. 5, 318–323.

Boardman, J.W., Kruse, F.A., 1994. Automated spectral analysis: a geologic example

using AVIRIS data. In: Proceedings ERIM Tenth Thematic Conference on Geologic Remote Sensing. Environmental Research Institute of Michigan, Ann Arbor, Michigan, pp. 407–418.
Boström, C., Jackson, E.L., Simenstad, C.A., 2006. Seagrass landscapes and their effects on associated fauna: a review. Estuar. Coast. Shelf Sci. 68, 383–403.
Boström, C., Pittman, S.J., Simenstad, C., Kneib, R.T., 2011. Seascape ecology of coastal biogenic habitats: advances, gaps, and challenges. Mar. Ecol. Prog. Ser. 427, 191–217.
Boyd, D.S., Foody, G.M., 2011. An overview of recent remote sensing and GIS based research in ecological informatics. Ecol. Inf. 6, 25–36.
Brandt, J.S., Townsend, P.A., 2006. Land use- land cover conversion, regeneration and degradation in the high elevation Bolivian Andes. Landsc. Ecol. 21, 607–623.
Carroway, R.J., Priddy, L.J., 1983. Mapping of Submerged Grass Beds in Core and Bogue Sounds, Carteret County, North Carolina, by Conventional Aerial Photography. CEIP Report No. 20. Coastal Energy Impact Program. Office of Coastal Management, North Carolina Department of Natural Resources and Community Development, Raleigh, North Carolina.
Congalton, R.G., 1991. A review of assessing the accuracy of classification of remotely sensed data. Remote Sens. Environ. 37, 35–46.
Congalton, R.G., Green, K., 2009. Assessing the Accuracy of Remotely Sensed Data: Principles and Practices, second ed. CRC Press, Boca Raton, Florida. 183 pp.
Congalton, R., Oderwald, R.G., Mead, R.A., 1983. Assessing Landsat classification accuracy using discrete multivariate statistical techniques. Photogramm. Eng. Remote Sens. 49, 1671–1678.
Conover, W.J., 1999. Practical Nonparametric Statistics, third ed. Wiley, Inc., New York.
Costello, C.T., Kenworthy, W.J., 2011. Twelve-year mapping and change analysis of eelgrass (*Zostera marina*) areal abundance in Massachusetts (USA) identifies statewide declines. Estuar. Coasts 34, 232–242.
den Hartog, C., 1971. The dynamic aspect in the ecology of seagrass communities. Thalass. Jugosl. 7, 101–112.
Dennison, W., Orth, R., Moore, K., Stevenson, J., Carter, V., Kollar, S., Bergstrom, P., Batiuk, R., 1993. Assessing water quality with submersed aquatic vegetation. BioScience 43, 86–95.
Dobson, J.E., Bright, E.A., Ferguson, R.L., Field, D.W., Wood, L.L., Haddad, K.D., Iredale III, H., Jensen, J.R., Klemas, V.V., Orth, R.J., Thomas, J.P., 1995. NOAA Coastal Change Analysis Program (C-CAP): Guidance for Regional Implementation. NOAA Technical Report NMFS 123. U.S. Department of Commerce, National Oceanic and Atmospheric Administration, Northwest Fisheries Science Center, Seattle, Washington.
Duran, O., Petrou, M., 2009. Spectral unmixing and superunity abundances for subpixel anomaly detection. IEEE Geosci. Remote Sens. Lett. 6, 152–156.
Ferguson, R.L., Korfmacher, K., 1997. Remote sensing and GIS analysis of seagrass meadows in North Carolina, USA. Aquat. Bot. 58, 241–258.
Ferguson, R.L., Wood, L.L., Graham, D.B., 1993. Monitoring spatial change in seagrass habitat with aerial photography. Photogramm. Eng. Remote Sens. 59, 1033–1038.
Field, D.W., 2007. Remote Sensing of Submerged Habitats in the Dry Tortugas: a Comparison of Multiple Sensors and Classification Techniques. Ph.D. thesis. University of South Carolina (Columbia, unpublished).
Finkbeiner, M., Stevenson, B., Seaman, R., 2001. Guidance for Benthic Habitat Mapping: an Aerial Photographic Approach. Technical Report NOAA/CSC/20117-PUB. U.S. Department of Commerce, National Oceanic and Atmospheric Administration, Coastal Services Center, Charleston, South Carolina.
Fisher, P., 1997. The pixel: a snare and a delusion. Int. J. Remote Sens. 18, 679–685.
Fitzpatrick-Lins, K., 1981. Comparison of sampling procedures and data analysis for a land- use and land-cover map. Photogramm. Eng. Remote Sens. 47, 343–351.
Fletcher, R.S., Pulich Jr., W., Hardegree, B., 2009. A semiautomated approach for monitoring landscape changes in Texas seagrass beds from aerial photography. J. Coast. Res. 25, 500–506.
Folkard, A.M., 2005. Hydrodynamics of model *Posidonia oceanica* patches in shallow water. Limnol. Oceanogr. 50, 1592–1600.
Fonseca, M.S., Bell, S.S., 1998. Influence of physical setting on seagrass landscapes near Beaufort, North Carolina, USA. Mar. Ecol. Prog. Ser. 171, 109–121.
Fonseca, M.S., Kenworthy, W.J., Griffith, E., Hall, M.O., Finkbeiner, M., Bell, S.S., 2008. Factors influencing landscape pattern of the seagrass *Halophila decipiens* in an oceanic setting. Estuar. Coast. Shelf Sci. 76, 163–174.
Fonseca, M.S., Kenworthy, W.J., Thayer, G.W., 1998. Guidelines for the Conservation and Restoration of Seagrasses in the United States and Adjacent Waters. NOAA Coastal Ocean Program Decision Analysis Series Number 12. NOAA Coastal Ocean Office, Silver Spring, Maryland, USA (accessed 22.12.15.). http://www.cop.noaa.gov/pubs/das/das12.pdf.
Fonseca, M.S., Kenworthy, W.J., Whitfield, P.E., 2000. Temporal dynamics of seagrass landscapes: a preliminary comparison of chronic and extreme disturbance events. Biol. Mar. Mediterr. 7, 373–376.
Fonseca, M.S., Zieman, J.C., Thayer, G.W., Fisher, J.S., 1983. The role of current velocity in structuring eelgrass (*Zostera marina* L.) meadows. Estuar. Coast. Shelf Sci. 17, 367–380.
Foody, G.M., 2002. Status of land cover classification accuracy assessment. Remote Sens. Environ. 80, 185–201.
Frazier, A.E., Wang, L., 2011. Evaluation of soft classifications for characterizing spatial patterns of invasive species. Remote Sens. Environ. 115, 1997–2007.
Gera, A., Pagès, J.F., Romero, J., Alcoverro, T., 2013. Combined effects of fragmentation and herbivory on *Posidonia oceanica* seagrass ecosystems. J. Ecol. 101, 1053–1061.
Goodman, J.A., Ustin, S.L., 2007. Classification of benthic composition in a coral reef environment using spectral unmixing. J. Appl. Remote Sens. 1, 501–518.
Green, A.A., Berman, M., Switzer, B., Craig, M.D., 1988. A transformation for ordering multispectral data in terms of image quality with implications for noise removal. IEEE Trans. Geosci. Remote Sens. 26, 65–74.
Green, K., Lopez, C., 2007. Using object-oriented classification of ADS40 data to map the benthic habitats of the state of Texas. Photogramm. Eng. Remote Sens. 73, 861–865.
Gustafson, E.J., 1998. Quantifying landscape spatial pattern: what is the state of the art? Ecosystems 1, 143–156.
Hamylton, S., 2011. Estimating the coverage of coral reef benthic communities from airborne hyperspectral remote sensing data: multiple discriminant function analysis and linear spectral unmixing. Int. J. Remote Sens. 32, 9673–9690.
Heck, K.L., Hays, G., Orth, R.J., 2003. Critical evaluation of the nursery role hypothesis for seagrass meadows. Mar. Ecol. Prog. Ser. 253, 123–136.
Hedley, J.D., Mumby, P.J., 2003. A remote sensing method for resolving depth and subpixel composition of aquatic benthos. Limnol. Oceanogr. 48, 480–488.
Holling, C.S., 1973. Resilience and stability of ecological systems. Annu. Rev. Ecol. Syst. 4, 1–23.
Holling, C.S., 1996. Surprise for science, resilience for ecosystems, and incentives for people. Ecol. Appl. 6, 733–735.
Ipe, D., 1987. Performing the Friedman test and the associated multiple comparison test using PROC GLM. In: Proceeding of the 12th Annual SAS Users Group International Conference. SAS Institute, Inc., Cary, North Carolina, pp. 1146–1148.
Jackson, E.L., Rees, S.E., Wilding, C., Attrill, M.J., 2015. Use of a seagrass residency index to apportion commercial fishery landing values and recreation fisheries expenditure to seagrass habitat service. Conserv. Biol. 29, 899–909.
Jackson, E.L., Rowden, A.A., Attrill, M.J., Bossey, S.J., Jones, M.B., 2001. The importance of seagrass beds as a habitat for fishery species. Oceanogr. Mar. Biol. Annu. Rev. 39, 269–303.
Jensen, J.R., 2005. Introductory Digital Image Processing: a Remote Sensing Perspective, third ed. Prentice Hall, Upper Saddle River, New Jersey.
Jensen, J.R., 2006. Remote Sensing of the Environment: an Earth Resource Perspective, second ed. Prentice Hall, Upper Saddle River, New Jersey.
Keane, R.E., Hessburg, P.F., Landres, P.B., Swanson, F.J., 2009. The use of historical range and variability (HRV) in landscape management. For. Ecol. Manag. 258, 1025–1037.
Kéfi, S., Guttal, V., Brock, W.A., Carpenter, S.R., Ellison, A.M., Livina, V.N., Seekell, D.A., Scheffer, M., van Nes, E.H., Dakos, V., 2014. Early warning signals of ecological transitions: methods for spatial patterns. PLoS One 9 (3), e92097. http://dx.doi.org/10.1371/journal.pone.0092097.
Kenworthy, W.J., 1981. The Interrelationship between Seagrass *Zostera Marina* and *Halodule Wrightii*, and the Physical and Chemical Properties of Sediments in a Mid-Atlantic Coastal Plain Estuary Near Beaufort, North Carolina. MSc. thesis. University of Virginia, Charlottesville, VA, 114 p.
Koch, E.W., Ackerman, J.D., Verduin, J., van Keulen, M., 2006. Fluid dynamics in seagrass ecology – from molecules to ecosystems. In: Larkum, A.W.D., Orth, R.J., Duarte, C.M. (Eds.), Seagrasses: Biology, Ecology and Conservation. Springer, Dordrecht, The Netherlands, pp. 193–225.
Landis, J., Koch, G., 1977. The measurement of observer agreement for categorical data. Biometrics 33, 159–174.
Lathrop, G., Montesano, P., Haag, S., 2006. A multi-scale segmentation approach to mapping seagrass habitats using airborne digital camera imagery. Photogramm. Eng. Remote Sens. 72, 665–675.
Lyzenga, D.R., 1978. Passive remote sensing techniques for mapping water depth and bottom features. Appl. Opt. 17, 379–383.
Lyzenga, D.R., 1981. Remote sensing of bottom reflectance and water attenuation parameters in shallow water using aircraft and Landsat data. Int. J. Remote Sens. 2, 71–82.
Marbà, N., Duarte, C.M., 1995. Coupling of seagrass (*Cymodocea nodosa*) patch dynamics to subaqueous dune migration. J. Ecol. 83, 381–389.
Maritorena, S., Morel, A., Gentili, B., 1994. Diffuse reflectance of oceanic shallow waters: influence of water depth and albedo. Limnol. Oceanogr. 39, 1689–1703.
Mather, P.M., 1999. Landcover classification revisited. In: Atkinson, P.M., Tate, N. (Eds.), Advances in Remote Sensing and GIS Analysis. John Wiley & Sons, Ltd, West Sussex, United Kingdom, pp. 7–16.
McGarigal, K., Ene, E., 2013. FRAGSTATS: a Spatial Pattern Analysis Program for Categorical Maps, Version 4.2. University of Massachusetts, Amherst. http://www.umass.edu/landeco/research/fragstats/fragstats.html.
Meehan, A.J., Williams, R.J., Watford, F.A., 2005. Detecting trends in seagrass abundance using aerial photograph interpretation: problems arising with the evolution of mapping methods. Estuaries 28, 462–472.
Meyer, C.A., 2008. Application of Remote Sensing Methods to Assess the Spatial Extent of the Seagrass Resource in St. Joseph Sound and Clearwater Harbor, Florida, U.S.A. Masters thesis. University of South Florida, St. Petersburg (unpublished).
Mobley, C.D., Sundman, L.K., Davis, C.O., Bowles, J.H., Downes, T.V., Leathers, R.A., Montes, M.J., Bisset, W.P., Kohler, D.D.R., Reid, R.P., Louchard, E.M., Gleason, A., 2005. Interpretation of hyperspectral remote-sensing imagery by spectrum matching and look- up tables. Appl. Opt. 44, 3576–3592.
Moore, K.A., Wilcox, D.J., Orth, R.J., 2000. Analysis of abundance of submersed aquatic vegetation communities in the Chesapeake Bay. Estuaries 23, 115–127.
Mount, R., 2006. Small Format Digital Aerial Photography for Mapping and Monitoring Seagrass Habitats in Shallow Temperate Marine Waters. Ph.D. thesis.

University of Tasmania, Australia (unpublished).
Page, E.B., 1963. Ordered hypotheses for multiple treatments: a significance test for linear ranks. J. Am. Stat. Assoc. 58, 216–230.
Patriquin, D.G., 1975. 'Migration' of blowouts in seagrass beds at Barbados and Carriacou, West Indies and its ecological and geological applications. Aquat. Bot. 1, 163–189.
Pech, R.P., Davies, A.W., Lamacraft, R.R., Graetz, R.D., 1986. Landsat data for sparsely vegetated semi-arid rangelands. Int. J. Remote Sens. 7, 1729–1750.
Peterson, C.H., Fodrie, J., Summerson, H.C., Powers, S.P., 2001. Site-specific and density-dependent extinction of prey by schooling rays: generation of a population sink in top-quality habitat for bay scallops. Oecologia 129, 349–356.
Pu, R., Bell, S., Meyer, C., 2014. Mapping and assessing seagrass bed changes in Central Florida's west coast using multitemporal Landsat TM imagery. Estuar. Coast. Shelf Sci. 149, 68–79.
Robbins, B.D., Bell, S.S., 2000. Dynamics of a subtidal seagrass landscape: seasonal and annual change in relation to water depth. Ecology 81, 1193–1205.
Roberts, D.A., Adams, J.B., Smith, M.O., 1993. Discriminating green vegetation, nonphotosynthetic vegetation and soils in AVIRIS data. Remote Sens. Environ. 44, 255–269.
Rohmann, S.O., Monaco, M.E., 2005. Mapping Southern Florida's Shallow-water Coral Ecosystems: an Implementation Plan. NOAA Technical Memorandum NOS NCCOS 19. U.S. Department of Commerce, National Oceanic and Atmospheric Administration, Center for Coastal Monitoring and Assessment, Silver Spring, Maryland.
Scheffer, M., Carpenter, S.R., 2003. Catastrophic regime shifts in ecosystems: linking theory to observation. TRENDS Ecol. Evol. 18, 648–656.
Schowengerdt, R.A., 2006. Remote Sensing: Models and Methods for Image Processing, third ed. Academic Press, Waltham, Massachusetts, p. 560.
Settle, J.J., Drake, N.A., 1993. Linear mixing and the estimation of ground cover proportions. Int. J. Remote Sens. 14, 1159–1177.
Smith, M.O., Johnson, P.E., Adams, J.B., 1985. Quantitative determination of mineral types and abundances from reflectance spectra using principal components analysis. Proceedings of the Fifteenth Lunar and Planetary Science Conference, Part 2. J. Geophys. Res. 90, 797–804.
Story, M., Congalton, R., 1986. Accuracy assessment: a user's perspective. Photogramm. Eng. Remote Sens. 52, 397–399.
Swetnam, T.W., Allen, C.D., Betancourt, J.L., 1999. Applied historical ecology: using the past to manage for the future. Ecol. Appl. 9, 1189–1206.
Thayer, G.W., Kenworthy, W.J., Fonseca, M.S., 1984. The Ecology of Eelgrass Meadows of the Atlantic Coast: a Community Profile. FWS/OBS-84/02. U.S. Fish and Wildlife Service, Washington D.C, 147 pp.
Thomlinson, J.R., Bolstad, P.V., Cohen, W.B., 1999. Coordinating methodologies for scaling landcover classifications from site-specific to global: steps toward validating global map products. Remote Sens. Environ. 70, 16–28.
Torres-Madronero, M.C., Velez-Reyes, M., Goodman, J.A., 2009. Underwater unmixing and water optical properties retrieval using HyCIAT. In: Shen, S.S., Lewis, P.E. (Eds.), Proceedings of SPIE. The International Society for Optics and Photonics, San Diego, California, 74570I-74571I-74570I-12.
Townsend, E.C., Fonseca, M.S., 1998. Bioturbation as a potential mechanism influencing spatial heterogeneity of North Carolina seagrass beds. Mar. Ecol. Prog. Ser. 169, 123–132.
Turner, S.J., Hewitt, J.E., Wilkinson, M.R., Morrisey, D.J., Thrush, S.F., Cummings, V.J., Funnell, G., 1999. Seagrass patches and landscapes: the influence of wind-wave dynamics and hierarchical arrangements of spatial structure on macrofaunal seagrass communities. Estuaries 22, 1016–1032.
Walker, D.I., Kendrick, G.A., McComb, A.J., 2006. Decline and recovery of seagrass ecosystems: the dynamics of change. In: Larkum, A.W.D., Orth, R.J., Duarte, C.M. (Eds.), Seagrasses: Biology, Ecology and Conservation. Springer, Dordrecht, The Netherlands, pp. 551–565.
Werdell, P.J., Roesler, C.S., 2003. Remote assessment of benthic substrate composition in shallow waters using multispectral reflectance. Limnol. Oceanogr. 48, 557–567.
Williams, A.P., Hunt, E.R., 2002. Estimation of leafy spurge cover from hyperspectral imagery using mixture tuned matched filtering. Remote Sens. Environ. 82, 446–456.
Woodcock, C.E., Strahler, A.H., 1987. The factor of scale in remote sensing. Remote Sens. Environ. 21, 311–332.
Young, D., Clinton, P., Specht, D., 2010. Mapping intertidal eelgrass (*Zostera marina* L.) in three coastal estuaries of the Pacific Northwest USA using false colour near-infrared aerial photography. Int. J. Remote Sens. 31, 1699–1715.
Zhang, C., Selch, D., Xie, Z., Roberts, C., Cooper, H., Chen, G., 2013. Object-based habitat mapping in the Florida Keys from hyperspectral imagery. Estuar. Coast. Shelf Sci. 134, 88–97.
Zoffoli, M.L., Frouin, R., Kampel, M., 2014. Water column correction for coral reef studies by remote sensing. Sensors 14, 16881–16931. http://dx.doi.org/10.3390/s140916881.